

# Quantum Kernel Principal Components Analysis for Compact Readout of Chemiresistive Sensor Arrays

Zheng Wang<sup>1,2,†</sup>, Timothy van der Laan<sup>2</sup>, and Muhammad Usman<sup>1,3</sup>

---

<sup>1</sup>Data61, CSIRO, Clayton, VIC 3168, Australia

<sup>2</sup>Manufacturing, CSIRO, West Lindfield, NSW 2070, Australia

<sup>3</sup>School of Physics, The University of Melbourne, Parkville, VIC 3010, Australia

† Corresponding author. Email: [zenwang@outlook.com](mailto:zenwang@outlook.com)

---

Keywords: Quantum computing; Quantum PCA; Quantum Machine Learning; Chemiresistive sensor; IoT

## Abstract

The rapid growth of Internet of Things (IoT) devices necessitates efficient data compression techniques to handle the vast amounts of data generated by these devices. In this context, chemiresistive sensor arrays (CSAs), a simple-to-fabricate but crucial component in IoT systems, generate large volumes of data due to their simultaneous multi-sensor operations. Classical principal component analysis (cPCA) methods, a common solution to the data compression challenge, face limitations in preserving critical information during dimensionality reduction. In this study, we present quantum principal component analysis (qPCA) as a superior alternative to enhance information retention. Our findings demonstrate that qPCA outperforms cPCA in various back-end machine-learning modeling tasks, particularly in low-dimensional scenarios when limited Quantum bits (qubits) can be accessed. These results underscore the potential of noisy intermediate-scale quantum (NISQ) computers, despite current qubit limitations, to revolutionize data processing in real-world IoT applications, particularly in enhancing the efficiency and reliability of CSA data compression and readout.

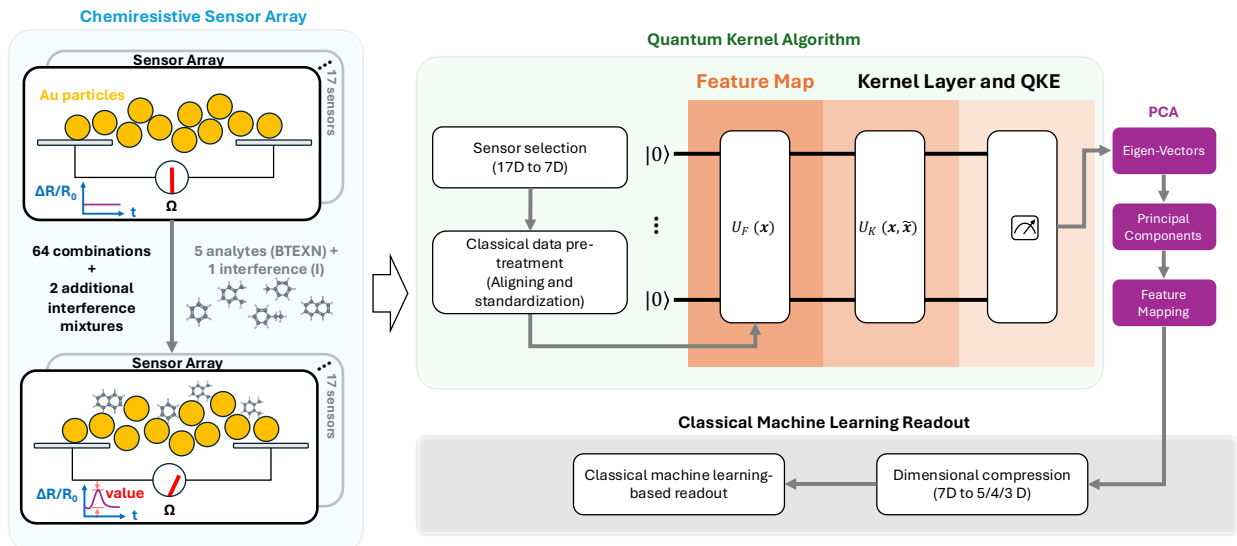


Fig. 1: Schematic illustration of the data processing procedure, emphasizing quantum PCA. The chemiresistive sensor array (CSA) consists of 17 sensors, and data were collected from the 7 most sensitive sensors for detecting 5 analytes and 1 interference mixture (see Methods). The data processing involves classical data pre-treatment, including aligning and standardizing the data. The quantum kernel algorithm comprises feature mapping  $U_F(\mathbf{x})$  which transforms classical data into a quantum state space, and kernel estimation  $U_K(\mathbf{x}, \tilde{\mathbf{x}})$  using Qiskit's sampling function to compute quantum fidelities. Quantum and Classical Principal component analysis (qPCA/cPCA) was then performed to extract principal components and achieve dimensionality reduction from 7D to lower dimensions (5D/4D/3D). The data with reduced dimensions is then used for classical machine learning (ML)-based readout.

Quantum computing (QC) is increasingly recognized as a pivotal solution for computationally intensive problems such as integer factorization<sup>1,2</sup> and quantum system simulations<sup>3,4</sup>. Likewise, it is anticipated that the integration of quantum computing in machine learning (ML) and data processing tasks will offer computational advantages such as speed-up<sup>5</sup>, enhanced accuracy<sup>6</sup>, and superior robustness<sup>7</sup>, made possible by unique quantum properties like superposition and entanglement. These properties allow data to be stored and processed in a potentially high-dimensional quantum space, leading to computation optimization<sup>8</sup>. Quantum machine learning (QML) has already demonstrated high potential in various applications. For instance, a hybrid classical-quantum principal component analysis (PCA) has been applied in drug design<sup>9</sup>, while other studies have explored quantum computing applications in finance and enhanced classical machine learning<sup>10, 11</sup>. Additionally, it has been theoretically predicted that quantum kernel methods could consistently outperform classical counterparts in modeling data with group structure<sup>8</sup>.

However, experimental research leveraging QML to solve real-world problems by identifying group structures in datasets has not yet been extensively carried out, leaving this theoretical work<sup>8</sup> largely unvalidated. Simultaneously, in noisy intermediate-scale quantum (NISQ) systems, practical applications of QML are becoming increasingly feasible<sup>12-15</sup>. Despite recent advancements in high-density QC architectures, the number of logical qubits in QC processors still falls short of demonstrating a significant quantum advantage<sup>16-19</sup>. This gap presents a unique opportunity to apply QML for practical problem-solving, particularly in enhancing data compression and readout compactness, when the number of qubits is a critical limitation. To address these challenges, this study employs a quantum kernel-based algorithm, quantum PCA (qPCA), to compress data and enhance backend data processing and therefore bridges the gap by demonstrating the practical utility of qPCA in IoT data compression, a real-world application. The experimental data used in this work was obtained from chemiresistive sensor arrays (CSAs), an example of a widely used IoT device due to their fabrication

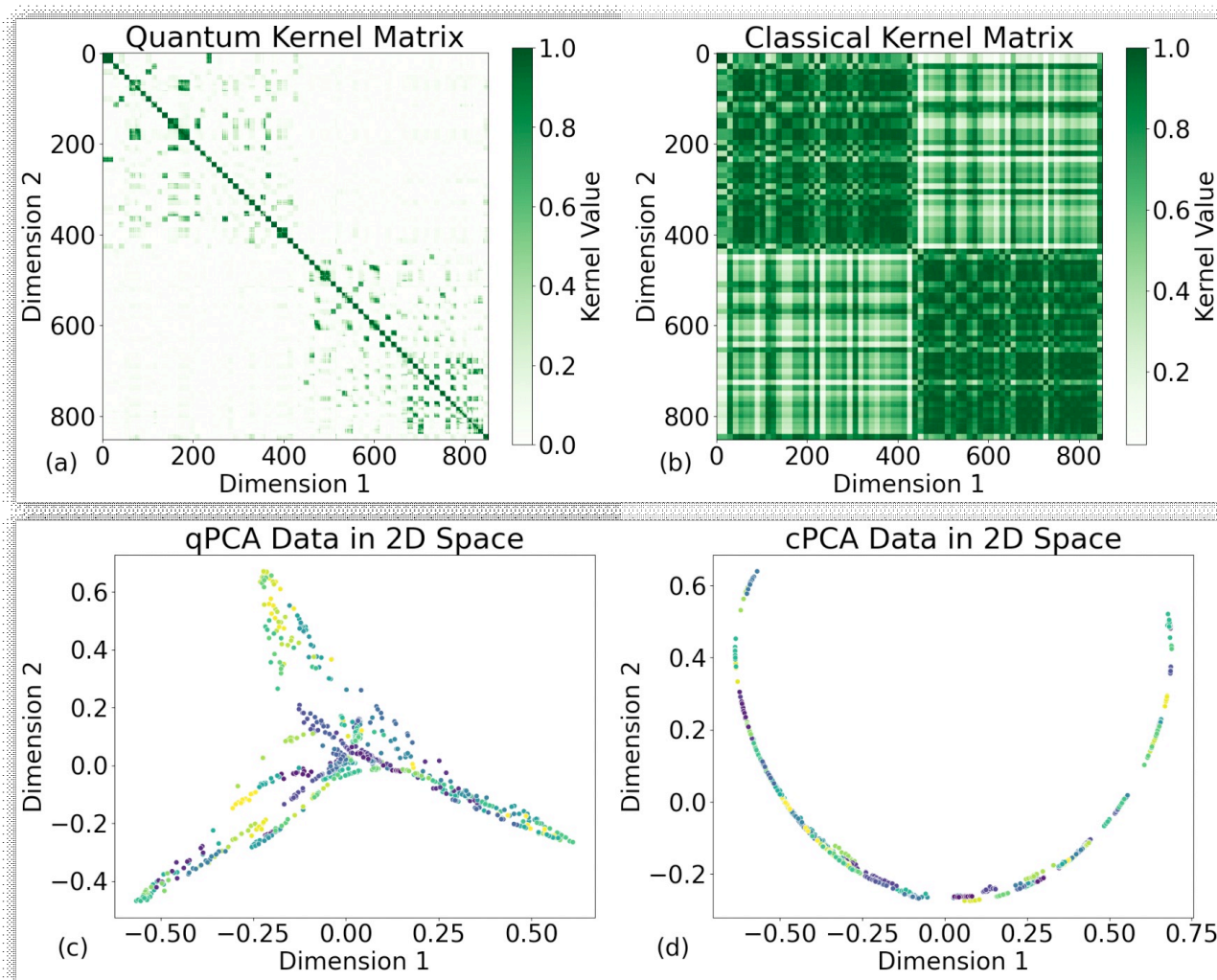


Fig. 2: Comparison of Quantum and Classical kernel matrices and their 2D mapping. (a) The quantum kernel matrix is based on the fidelity between quantum states. It exhibits a scattered and irregular pattern, indicating complex relationships captured in the quantum feature space, with darker regions signifying higher similarity between data points. (b) The classical kernel matrix uses a radial basis function (RBF) kernel, displaying a more uniform and regular pattern with distinct dark stripes, indicating simpler relationships and higher similarity within certain dimensions. The differences, particularly in the off-diagonal regions, illustrate how quantum kernels can capture more nuanced and potentially non-linear relationships compared to classical kernels. (c) qPCA and (d) cPCA 2D visualization of the compressed data. The data were visualized using t-SNE embedding after dimensionality reduction. (c) The qPCA projection shows a dispersed cluster of points, reflecting the nuanced relationships captured by the quantum kernel. (d) The cPCA projection reveals a more defined curve, indicating that the classical kernel emphasizes dominant features of the data but may lose structural information during dimensional reduction. The distinct patterns demonstrate the differing capabilities of qPCA and cPCA in retaining complex data structures.

simplicity, high sensitivity, and specificity in detecting chemical changes. However, CSAs generate large volumes of data due to their requirement for multiple sensors to operate simultaneously, posing significant challenges for data compression and processing. While classical compression techniques have been developed<sup>20-23</sup>, these methods often struggle with

maintaining data integrity during the reduction process, leading to loss of critical information<sup>24</sup>. Our findings demonstrate that qPCA outperforms classical PCA (cPCA) in preserving critical information during dimensionality reduction, leading to more efficient and reliable data modeling.

This manuscript discusses the integration of QML with

real-world data challenges, making a case for the adoption of quantum methods in broader contexts beyond theoretical applications. As shown in Fig. 1, in this study, we employ quantum qPCA to achieve compact readout of CSA data. We utilized a fidelity-based quantum kernel to map readings from seven sensors into quantum state space and then compress the data by reducing the dimension of that space. Following dimensional reduction, we applied various classical ML (CML) algorithms to determine the readout results. Compared to the classical kernel (radio-basis function kernel, RBFK), our quantum fidelity kernel (QFK) demonstrated lower information loss, leading to enhanced ML-based readout accuracy, which has only been theorized previously<sup>8</sup>.

## Quantum and classical kernels

Fig. 2 presents a side-by-side comparison of the quantum, Fig. 2(a), and classical, Fig. 2(b), kernel matrices. The quantum kernel matrix, characterized by a scattered and irregular pattern of darker blocks, indicates a high degree of similarity between certain groups of data points. This suggests the quantum kernel can capture complex, potentially non-linear relationships within the data in the quantum feature space. In contrast, the lighter, white areas indicate near-zero similarity, implying independence or irrelevance between the data points in these regions.

The classical kernel matrix displays a more uniform and regular pattern, with dark stripes signifying dimensions where data points share higher similarity. This pattern may suggest that relationships in the classical feature space are simpler, and that the classical kernel emphasizes certain dominant features of the data. The stark differences between the two matrices illustrate how various kernel functions capture the intrinsic structure of the data. The quantum kernel may be sensitive to more subtle or complex relationships, whereas the classical kernel might highlight broader, more significant features<sup>25</sup>.

## Quantum PCA-based data compression

Utilizing the quantum kernel the 7D data can be compressed into 6/5/4/3D space. Fig. 2, the 2D

visualization (t-SNE embedding) of data compressed by qPCA (c) and cPCA (d) allows for another comparison of the two methods. The qPCA projection shows a dispersed cluster of points, possibly reflecting the nuanced relationships that the quantum kernel captures. Meanwhile, the cPCA projection reveals a more defined curve, indicating that the classical kernel may be distilling the data into a form that reflects its main features with clear separation. However, this means that the data loses its structural information during the dimensional reduction. It should be noted that, however, the ultimate choice of kernel for a given task should not rely solely on visual inspection; it must be informed by empirical performance metrics, such as classification accuracy, regression error, or other relevant benchmarks in machine learning models.

## Classical machine learning readout

To delve into the nuances of how qPCA and cPCA influence information retention during dimensionality reduction. We applied five different ML algorithms to predict the chemical types that the CRS detected in different samples. Each algorithm serves as a probe into the kernels' efficacy. As delineated in Fig. 3, data refined through qPCA were more amenable to modeling by these algorithms, evidenced by their generally higher evaluation scores. Nonetheless, it is imperative to acknowledge the conditions under which cPCA-treated data surpassed qPCA's performance. A notable instance is observed with dimensions above 5D for the RF algorithm, where cPCA maintained higher scores. This suggests that cPCA can preserve certain intricate non-linear patterns within the original dataset, which RF can exploit to garner additional insights. This preservation of complex structures, however, seems to diminish rapidly with further dimensional reduction, as demonstrated by the comparative analysis within the RF subfigures in Fig. 3.

Examining the lower-dimensional performance of linear-based algorithms, such as LC and L-SVM, we also see cPCA perform better than qPCA, as shown in Fig. 3 (p), (q), (u), and (v). Despite cPCA's use of the inherently non-linear RBF kernel, this phenomenon indicates preferential retention of linear-like patterns

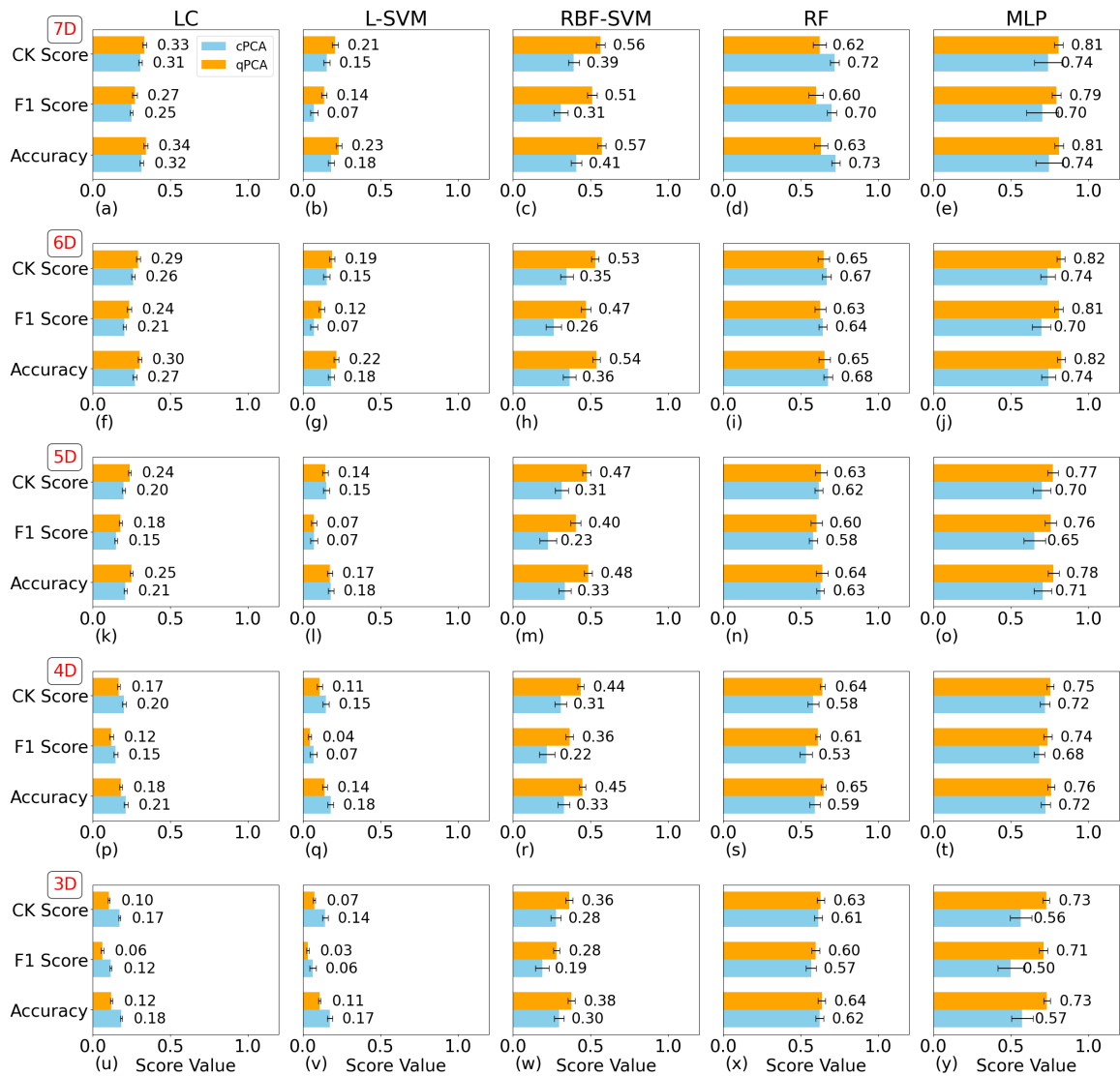


Fig. 3: Evaluation scores of each model in different data spaces using classical cPCA (in blue) and qPCA (in yellow). The performance of five machine learning models (LC, L-SVM, RBF-SVM, RF, MLP) is evaluated across various reduced dimensions (7D, 6D, 5D, 4D, 3D). Panels (a)-(e) show results for 7D, (f)-(i) for 6D, (k)-(o) for 5D, (p)-(t) for 4D, and (u)-(y) for 3D. The orange bars represent scores from qPCA-treated data, while the blue bars represent scores from cPCA-treated data. Each subfigure displays three evaluation metrics: CK Score, F1 Score, and Accuracy. The PCA-based dimensional reduction process remains consistent across both cPCA and qPCA, with the primary difference being the kernel-based mapping. Results indicate that qPCA generally outperforms cPCA in preserving critical information during dimensional reduction in non-linear ML-based readout, leading to higher evaluation scores across most models and dimensions.

through the dimensionality reduction process. The qPCA may be overlooking linear patterns during dimensionality reduction hence the lower scores compared to the cPCA. However, we observe that the scores for both cPCA and qPCA methods, as well as for LC and L-SVM, are generally low, indicating that the linear-like patterns represent only a small portion of the overall data. In addition, the low scores may indicate that while the cPCA method preserves linear patterns during the dimensionality reduction, it could

be omitting nonlinear patterns in the data. Conversely, the quantum PCA (qPCA) method is more adept at retaining nonlinear patterns. This suggests that qPCA could be particularly effective for data dimension compression when the critical information within the data predominantly resides in nonlinear patterns.

It is however crucial to recognize that these linear patterns form only a fragment of the overall information necessary for robust modeling our CSA

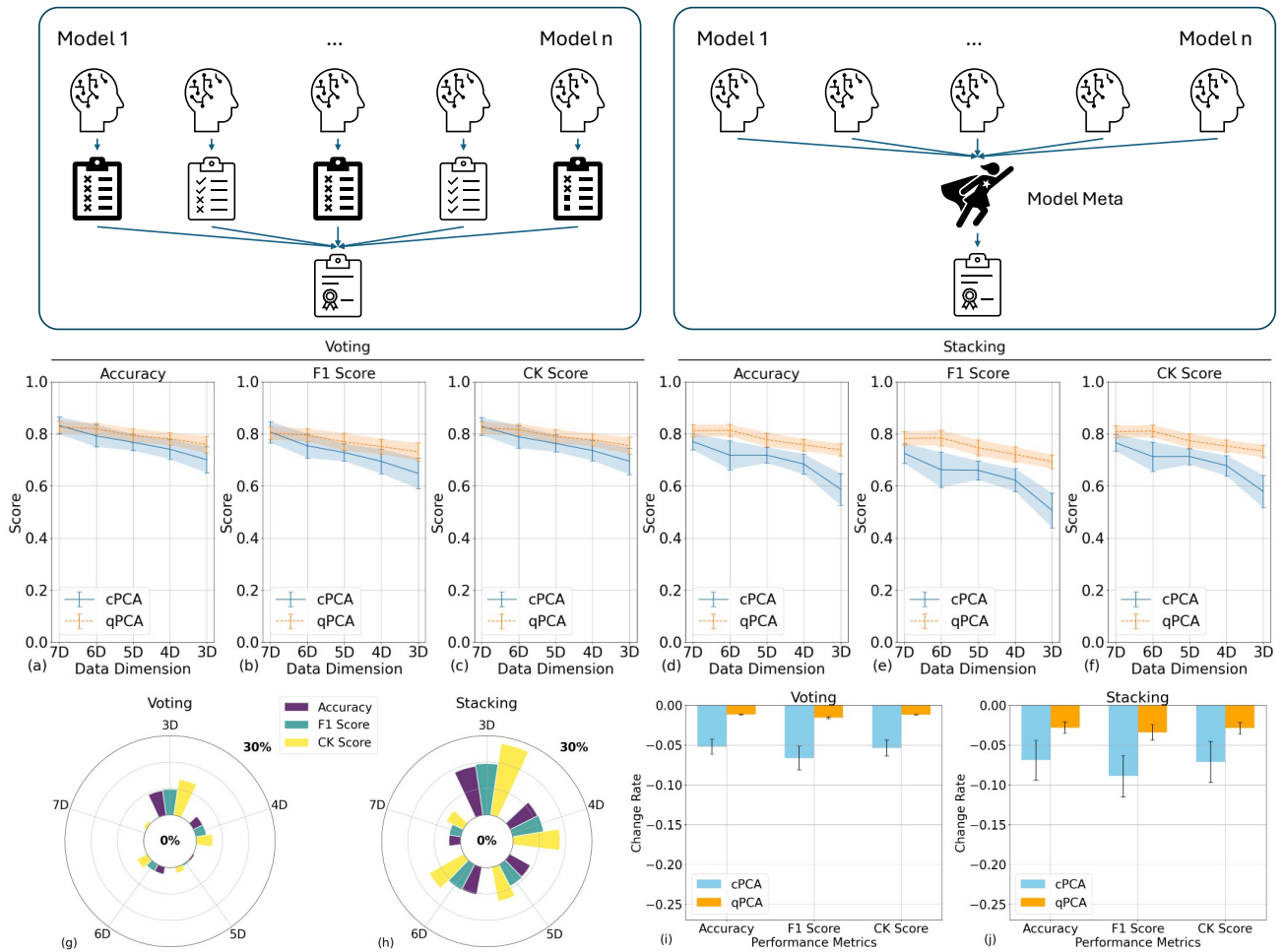


Fig. 4: Evaluation scores of cPCA and qPCA across shrinking dimensions using ensemble learning methods. The performance of two ensemble learning methods—(a)-(c) soft-voting and (b)-(d) stacking—was assessed by integrating five machine learning models into a single model. The lines represent the average scores, while the shaded areas indicate the variances. For both methods, three evaluation metrics (Accuracy, F1 Score, and CK Score) were compared between cPCA and qPCA across different reduced dimensions (7D, 6D, 5D, 4D, 3D). Results show that qPCA consistently achieves higher scores than cPCA, with a more gradual decline in performance as the data dimension decreases, indicating better preservation of essential information during dimensionality reduction. (g)-(h): Improvement percentage (quantum improvement) between the ML evaluation scores of qPCA and cPCA-treated data across different dimensions. The improvement percentage is calculated as  $(\text{qPCA score} - \text{cPCA score}) / \text{cPCA score} * 100\%$  for three metrics: Accuracy, CK Score, and F1 Score. (g) The voting ensemble method and (h) the stacking ensemble method show that qPCA provides relatively higher information retention in more compressed spaces (4D and 3D), demonstrating significant performance gains over cPCA as the dimensionality reduces. This indicates the superior capability of qPCA in preserving critical information during dimensional reduction. (i)-(j): Change rates of the evaluation scores averaged from 7D to 3D. The change rates for Accuracy, F1 Score, and CK Score are shown for both (i) voting and (j) stacking ensemble methods. The blue bars represent the cPCA scores, and the orange bars represent the qPCA scores. The results indicate that the averaged change rates of all three metrics are lower for qPCA compared to cPCA, demonstrating that qPCA retains information more effectively across dimensionality reduction, resulting in more stable performance metrics.

data. This is substantiated when juxtaposing the performance metrics of linear and non-linear models, the latter typically presents higher scores., While cPCA

occasionally demonstrates advantageous outcomes, particularly in partially preserving linear components and certain non-linear patterns beneficial to

algorithms like RF in uncompressed space, the overarching data narrative attests to the superior comprehensive capability of qPCA.

## Benchmarking qPCA and cPCA

The results portrayed in Fig. 4 reinforce the assertion that qPCA outperforms cPCA in compressing the data from the CSA-based IoT system studied. These frameworks synergistically combine the predictive power of all five ML algorithms used, as shown in the upper panel of the figure. The analysis in Fig. 4(a)-(f) reveals that the qPCA-based models have a more gradual decline in performance scores relative to cPCA, as dimensionality decreases. This trend is consistent across both voting and stacking methods. This reinforces the robustness of qPCA in preserving essential information during the data compression process.

The sustained performance of qPCA in lower-dimensional spaces is indicative of its ability to maintain the integrity of multidimensional relationships, a quality that is vital for the complex task of IoT computation. Ensemble models built upon qPCA consistently outscore their cPCA counterparts, as shown in Fig. 4(g)-(h). No negative scores were found when comparing qPCA to cPCA in lower dimensions ( $< 6D$ , mean values), in either the stacking or voting ensembles. We do note however that this claim is within the margin of statistical uncertainty in all scenarios. This improvement in data quality retention as dimensionality is reduced is also seen in the rate at which the scores for different ensembles decrease with dimensionality reduction (the slope of the scores vs the dimensions) as shown in Fig. 4(i)-(j). Consistently we see that the score's change rate using qPCA are lower than the cPCA scores.

## Discussion

Recent advancements in quantum machine learning demonstrate the efficacy of quantum kernels in classifying data with inherent group structures<sup>8</sup>. Using our experimental dataset, this study demonstrates the effectiveness of quantum kernel methods and their potential for real-world applications. We provide

evidence that quantum kernel-based PCA offers promising solutions for complex data compression problems with non-obvious relationships. Particularly for processing from high to low dimensions, the proposed qPCA method shows promise, as applying quantum data processing using qubits has become feasible in the NISQ era.

While this study highlights qPCA's potential advantages over cPCA in our framework, it is yet to be determined whether qPCA universally outperforms all kernel-based cPCA methods. A carefully crafted kernel or tailored post-processing algorithm could enhance cPCA's ability to preserve critical information during dimensionality reduction. Moreover, implementing cPCA is straightforward with established algorithms and software support, allowing easy application with conventional computing resources. In contrast, qPCA requires higher computational demands and specialized quantum computing resources, reflecting its developmental stage.

## Summary and outlook

In conclusion, the findings of this study underscore the advantage of qPCA over cPCA for data compression in Internet of Things (IoT) applications. This work provides an experimental demonstration of the previous theoretical prediction of a quantum approach to dimensionality reduction in datasets<sup>8</sup>. Using only limited qubits, our experimental results demonstrate that qPCA appears to maintain key information through a dimensionality reduction process more effectively than cPCA, this is evidenced by consistently higher performance scores across a variety of machine learning (ML) models when using the compressed data. This is further emphasized when ensemble learning models are integrated within ensemble learning frameworks such as soft voting and stacking.

The propensity of qPCA to retain more informative features endorses its potential as the preferred

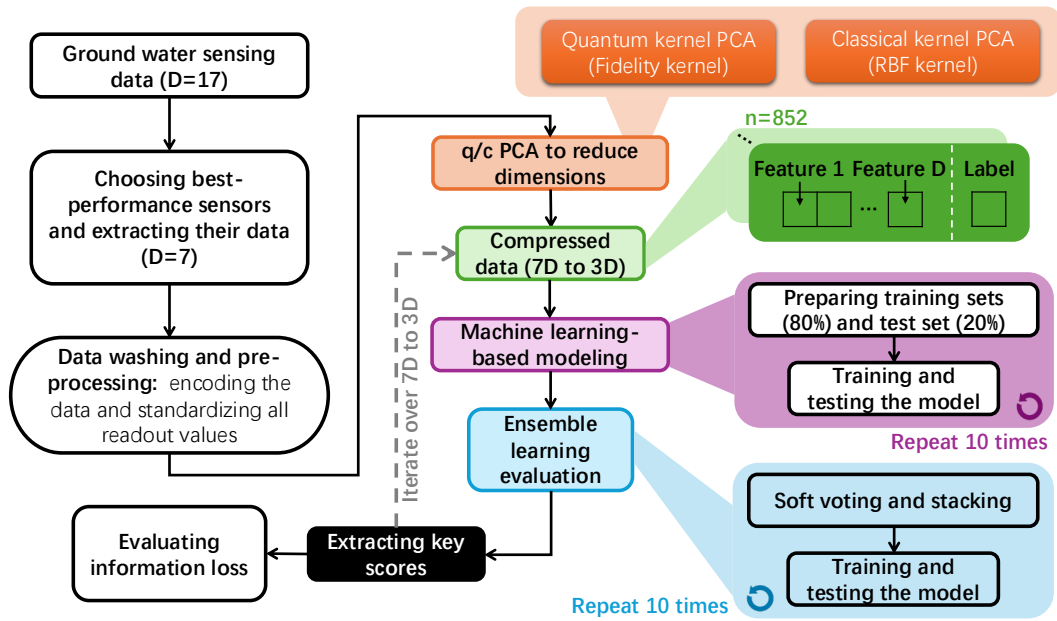


Fig. 5: Schematic flowline illustration of the procedure of this study. The process begins with the collection of groundwater sensing data using 17 sensors ( $D=17$ ). The best-performing sensors are selected, reducing the data to 7 dimensions ( $D=7$ ). The data is then washed and pre-processed by encoding and standardizing all readout values. Both quantum kernel PCA (fidelity kernel) and classical kernel PCA (RBF kernel) are applied to reduce the dimensions further (7D to 3D). The compressed data is then split into training (80%) and test (20%) sets. Machine learning-based modeling is performed, followed by training and testing the models. This process is repeated 10 times to ensure robustness. The ensemble learning evaluation is conducted using soft voting and stacking methods, which are also iterated 10 times to extract key scores and evaluate information loss. All evaluation results are averaged over the 10 repetitions to ensure reliability.

technique for sophisticated data-compression tasks in IoT systems. Future research may explore the application potential of qPCA across diverse data types and tasks, as well as the optimization of qPCA kernels to adapt different structures of data processing in quantum computers of the NISQ era. It is also worthwhile to explore the deployment of QML models on commercially available quantum computers.

## Methods

**Experimental data:** In this study, we sourced our sensing data from the dataset detailed in Ref<sup>26</sup>. This dataset comprises readings from 17 sensors across 852 experiments (data shape:  $852 \times 17$ ), with each 17-dimensional data point linked to one of 66 labels identifying the detected chemical. Due to the qubit limitations inherent in NISQ systems, we initially narrowed our focus to data from seven specific sensors (4-BBM, 1-2-BDMT, MOB, 3-ETP, 4-MBT, 4-

CBT), resulting in a refined dataset of 852 experiments, each with 7-dimensional readings (selected data shape:  $852 \times 7$ ). Each data item consisted of these 7D readings paired with a label. The whole procedure of the data processing and analysis can be found in Fig. 5. The experimental setup for collecting the CSA data is briefly illustrated in the left panel of Fig. 1 and more details about the sensor's fabrication and the wet experiments can be found in our previous work<sup>26</sup>.

For data compression, we employed kernel PCA utilizing two distinct kernel functions: the Quantum Fidelity Kernel (QFK) and the Radio-Basis Function Kernel (RBFK).

**Quantum PCA:** Kernel PCA transforms the data into a higher dimensional space defined by a kernel function  $K$ , where  $K(x_i, x_j)$  represents the similarity between two points in the original space. The transformation is

given by:

$$\Phi(x) = K(\cdot, x) \quad (1)$$

In the case of QFK PCA, we use the quantum fidelity between quantum states, which is defined as:

$$F(\rho_i(x_i), \rho_j(x_j)) = \left( \text{Tr} \sqrt{\sqrt{\rho_i(x_i)} \rho_j(x_j) \sqrt{\rho_i(x_i)}} \right)^2 \quad (2)$$

Here,  $\rho_i(x_i)$  and  $\rho_j(x_j)$  are density matrices representing the quantum states mapped from the data. In this work, we adopted Pauli feature map function to realize the mapping from classical space to quantum state space<sup>27</sup>. The qubits were initialized to  $|0\rangle^7$  states to encode the CSA data. The fidelity measures the closeness between two quantum states, which in our context, serves as a measure of similarity between data points when transformed to quantum state space. We can define our kernel matrix  $K$  where each element  $K(x_i, x_j)$  is the fidelity between states  $\rho_i$  and  $\rho_j$ :

$$K(x_i, x_j) = F(\rho_i, \rho_j) = \left( \text{Tr} \sqrt{\sqrt{\rho_i} \rho_j \sqrt{\rho_i}} \right)^2 \quad (3)$$

The qPCA's procedure is illustrated in Fig. 5, where the quantum kernel estimation (QKE) was realized by the sampling function of Qiskit<sup>28</sup>. Following the QKE, the classical mapping algorithm was used to calculate the principal components and to realize the feature mapping, as shown in Fig. 5.

**Classical PCA:** For RBFK PCA, the kernel is defined by the Gaussian function:

$$K(x_i, x_j) = \exp\left(-\frac{|x_i - x_j|^2}{2\sigma^2}\right) \quad (4)$$

$\|x_i - x_j\|$  is the Euclidean distance between data points  $x_i$  and  $x_j$ , and  $\sigma$  is a free parameter that controls the width of the Gaussian.

Applying these kernel methods, we performed dimensionality reduction on the 7D data, mapping it into a feature space via a kernel function  $K$ . In this space, we computed the covariance matrix  $C$  defined by the kernel as:

$$C = \frac{1}{n} \sum_{i=1}^n (K \cdot \phi(x_i))(K \cdot \phi(x_i))^T \quad (5)$$

where  $n$  is the number of data samples,  $\phi(x_i)$  is the implicit mapping of the data point  $x_i$  by the kernel function  $K$ , and  $T$  denotes the transpose operation. We then solved the eigenvalue problem:

$$C \cdot v = \lambda \cdot v \quad (6)$$

where  $v$  are the eigenvectors and  $\lambda$  are the eigenvalues. The eigenvectors corresponding to the largest eigenvalues give us the principal components in the feature space. By selecting the top  $k$  eigenvectors, we can form a reduced feature space of dimension  $k$ , where  $k$  is less than the original dimensionality of the data. For our purposes, we chose  $k = 6, 5, 4,$  and  $3$  to obtain a 6D, 5D, 4D, and 3D representation of the data, respectively. In this reduced feature space, the transformed data points  $\hat{x}_i$  are given by:

$$\hat{x}_i = [v_1^T \cdot \phi(x_i), v_2^T \cdot \phi(x_i), \dots, v_k^T \cdot \phi(x_i)] \quad (7)$$

This transformation is expected to retain the essential features of the original data and to be suitable for processing within a NISQ environment due to the lower dimensionality. It is now evident that different mapping strategies, i.e. different  $K$  and  $\phi(x_i)$ , will lead to different transformed data points  $\hat{x}_i$ .

**Machine Learning Models:** Following the dimensional reduction, we evaluated the information retention in the compressed data using five Classical Machine Learning (CML) algorithms, including linear

classifier (LC), linear kernel support vector machine classifier (L-SVM), RBF kernel support vector machine classifier (RBF-SVM), random forests (RF), neural network (based on multiple-layer perceptron, MLP). The core methodologies of these CML algorithms encompass a broad spectrum, incorporating linear models, kernel methods, decision trees, and neural networks to provide a comprehensive range of modeling capabilities. For this evaluation, the datasets compressed via QFK and RBFK PCA were randomly split into training (80%) and testing (20%) sets, with stratified sampling. To ensure robustness in our results, we repeated this data splitting process 10 times, calculating the average evaluation scores over these iterations for each algorithm. We also avoided using calculated scores (e.g. accuracies and F1 scores) to directly derive the trend of reducing the data dimension. Instead, we calculated the scores again when obtaining the trend, in order to further enhance the robustness of the results.

To consolidate the strengths of all five CML models, we employed ensemble learning frameworks, including soft voting and stacking methods. These frameworks were utilized to integrate the results from the individual models – The final prediction was made by all the individual models by voting or stacking mechanism<sup>29</sup>. We then extracted key metrics — Accuracy, F1 score, and Cohen's Kappa (CK) score<sup>30</sup> — along with their rate of change across different dimensions, to illustrate the outcomes from the two ensemble learning frameworks.

For the implementation, we used Python 3.10, with ML models sourced from the Scikit-Learn package (version 1.4.0) and quantum ML models from Qiskit 0.44.1 and Qiskit-Machine-Learning 0.6.0<sup>28</sup>. All ML models' settings used the default settings directly. The kernels employed for this study were the fidelity kernel for quantum analysis and the RBF kernel for classical analysis. The code was executed on a computer

equipped with a Ryzen 5600G CPU and 16Gb of memory.

## Acknowledgements

This work was partially supported by CSIRO Impossible-Without-You program.

## References

1. Jiang, S., Britt, K. A., McCaskey, A. J., Humble, T. S. & Kais, S. Quantum Annealing for Prime Factorization. *Sci. Rep.* **8**, 17667 (2018).
2. Borders, W. A. *et al.* Integer factorization using stochastic magnetic tunnel junctions. *Nature* **573**, 390–393 (2019).
3. Boghosian, B. M. & Taylor, W. Simulating quantum mechanics on a quantum computer. *Phys. Nonlinear Phenom.* **120**, 30–42 (1998).
4. Zalka, C. Simulating quantum systems on a quantum computer. *Proc. R. Soc. Lond. Ser. Math. Phys. Eng. Sci.* **454**, 313–322 (1998).
5. Biamonte, J. *et al.* Quantum machine learning. *Nature* **549**, 195–202 (2017).
6. Cerezo, M., Verdon, G., Huang, H.-Y., Cincio, L. & Coles, P. J. Challenges and opportunities in quantum machine learning. *Nat. Comput. Sci.* **2**, 567–576 (2022).
7. West, M. T. *et al.* Towards quantum enhanced adversarial robustness in machine learning. *Nat. Mach. Intell.* **5**, 581–589 (2023).
8. Glick, J. R. *et al.* Covariant quantum kernels for data with group structure. *Nat. Phys.* (2024) doi:10.1038/s41567-023-02340-9.
9. Batra, K. *et al.* Quantum Machine Learning Algorithms for Drug Discovery Applications. *J. Chem. Inf. Model.* **61**, 2641–2647 (2021).
10. Orús, R., Mugel, S. & Lizaso, E. Quantum computing for finance: Overview and prospects. *Rev. Phys.* **4**, 100028 (2019).
11. Perdomo-Ortiz, A., Benedetti, M., Realpe-Gómez, J. & Biswas, R. Opportunities and challenges for quantum-assisted machine learning in near-term quantum computers. *Quantum Sci. Technol.* **3**, 030502 (2018).
12. Cheng, B. *et al.* Noisy intermediate-scale quantum

- computers. *Front. Phys.* **18**, 21308 (2023).
13. Bharti, K. *et al.* Noisy intermediate-scale quantum algorithms. *Rev. Mod. Phys.* **94**, 015004 (2022).
  14. West, M. T. *et al.* Drastic Circuit Depth Reductions with Preserved Adversarial Robustness by Approximate Encoding for Quantum Machine Learning. Preprint at <https://doi.org/10.48550/ARXIV.2309.09424> (2023).
  15. West, M. T., Seviar, M. & Usman, M. Boosted Ensembles of Qubit and Continuous Variable Quantum Support Vector Machines for B Meson Flavor Tagging. *Adv. Quantum Technol.* **6**, 2300130 (2023).
  16. Strikis, A., Benjamin, S. C. & Brown, B. J. Quantum Computing is Scalable on a Planar Array of Qubits with Fabrication Defects. *Phys. Rev. Appl.* **19**, 064081 (2023).
  17. Liu, Y., Guan, S., Luo, J. & Li, S. Progress of Gate-Defined Semiconductor Spin Qubit: Host Materials and Device Geometries. *Adv. Funct. Mater.* 2304725 (2024) doi:10.1002/adfm.202304725.
  18. Dalzell, A. M., Harrow, A. W., Koh, D. E. & La Placa, R. L. How many qubits are needed for quantum computational supremacy? *Quantum* **4**, 264 (2020).
  19. Harrow, A. W. & Montanaro, A. Quantum computational supremacy. *Nature* **549**, 203–209 (2017).
  20. Li, S., Xu, L. D. & Wang, X. Compressed Sensing Signal and Data Acquisition in Wireless Sensor Networks and Internet of Things. *IEEE Trans. Ind. Inform.* **9**, 2177–2186 (2013).
  21. Pudlewski, S., Prasanna, A. & Melodia, T. Compressed-Sensing-Enabled Video Streaming for Wireless Multimedia Sensor Networks. *IEEE Trans. Mob. Comput.* **11**, 1060–1072 (2012).
  22. Fazel, F., Fazel, M. & Stojanovic, M. Random Access Compressed Sensing for Energy-Efficient Underwater Sensor Networks. *IEEE J. Sel. Areas Commun.* **29**, 1660–1670 (2011).
  23. Palopoli, L., Passerone, R. & Rizano, T. Scalable Offline Optimization of Industrial Wireless Sensor Networks. *IEEE Trans. Ind. Inform.* **7**, 328–339 (2011).
  24. Nassra, I. & Capella, J. V. Data compression techniques in IoT-enabled wireless body sensor networks: A systematic literature review and research trends for QoS improvement. *Internet Things* **23**, 100806 (2023).
  25. Ghukasyan, A., Baker, J. S., Goktas, O., Carrasquilla, J. & Radha, S. K. Quantum-Classical Multiple Kernel Learning. Preprint at <https://doi.org/10.48550/ARXIV.2305.17707> (2023).
  26. Cooper, J. S. *et al.* Quantifying BTEX in aqueous solutions with potentially interfering hydrocarbons using a partially selective sensor array. *The Analyst* **140**, 3233–3238 (2015).
  27. Havlíček, V. *et al.* Supervised learning with quantum-enhanced feature spaces. *Nature* **567**, 209–212 (2019).
  28. Treinish, M. Qiskit/qiskit-metapackage: Qiskit 0.44.0. Zenodo <https://doi.org/10.5281/ZENODO.2573505> (2023).
  29. Mienye, I. D. & Sun, Y. A Survey of Ensemble Learning: Concepts, Algorithms, Applications, and Prospects. *IEEE Access* **10**, 99129–99149 (2022).
  30. Vieira, S. M., Kaymak, U. & Sousa, J. M. C. Cohen's kappa coefficient as a performance measure for feature selection. in *International Conference on Fuzzy Systems* 1–8 (IEEE, Barcelona, Spain, 2010). doi:10.1109/FUZZY.2010.5584447.